



# **SPUDNUT: A Transport Code for Neutral Atoms in Plasmas**

**K. Audenaerde, G.A. Emmert, and M. Gordinier**

**September 1978**

**UWFDM-259**

J. Comp. Phys. 34, 268 (1980).

***FUSION TECHNOLOGY INSTITUTE  
UNIVERSITY OF WISCONSIN  
MADISON WISCONSIN***

# **SPUDNUT: A Transport Code for Neutral Atoms in Plasmas**

K. Audenaerde, G.A. Emmert, and M. Gordinier

Fusion Technology Institute  
University of Wisconsin  
1500 Engineering Drive  
Madison, WI 53706

<http://fti.neep.wisc.edu>

September 1978

UWFDM-259

SPUDNUT: A Transport Code for Neutral Atoms in Plasmas

K. Audenaerde  
G. A. Emmert  
M. Gordinier

Department of Nuclear Engineering  
University of Wisconsin  
Madison, Wisconsin 53706

## ABSTRACT

The problem of neutral atom transport in plasmas is formulated in terms of an integral equation for the charge exchange collision density. This formulation is used as the basis for a numerical code, SPUDNUT, which is exceptionally fast and compact. Comparative calculations with other neutral particle transport codes are presented.

## 1. Introduction

It is well-known that neutral hydrogenic atoms play an important role in the evolution of tokamak discharges. Neutral atoms affect both the particle and energy balance of the plasma and, by wall bombardment, can erode the chamber wall as well as provide a mechanism for the generation of impurities which enter the plasma. Consequently, codes which calculate the transport of neutral atoms, are generally included as routines in tokamak simulation codes [1,2]. Furthermore, the energetic neutral particles emerging from the plasma are often used as a diagnostic of the plasma ion temperature and the quantity and energy of these neutrals are of interest to surface physicists.

Greenspan [3] pointed out that neutral particle transport is conceptually the same as photon or neutron transport. Consequently, neutronics codes, such as ANISN, can be easily adapted to neutral atom transport. Several calculations of this type have been reported [3-7]. Unfortunately such codes are bulky and slow since they are designed to treat complicated neutron interactions; the neutral atom processes in a plasma are rather simple in comparison. This simplicity has led to the development of special purpose neutral transport routines which are better suited for inclusion in tokamak simulation codes. Some of these special purpose routines have been discussed by Hogan [2] in his review. The role then of codes based on neutron transport methods has been to provide an accuracy standard for the special purpose routines [6,7].

We present here a special purpose neutral transport routine which is exceptionally compact and fast. This routine, which is designed for inclusion in tokamak simulation codes, is based on an integral equation

for neutral particle transport. The geometry is that of a finite thickness plasma slab with a source of neutral atoms at the plasma edge. For large tokamaks in which the neutral atom mean free path is much less than the minor radius, this assumption of slab geometry is sufficient for wall-originated neutrals. For neutrals originating near the center of the device (e.g., from beam injection), cylindrical effects are more important. In Sec. 2, we formulate the integral equation on which the neutral transport routine is based. This equation is then transformed in Sec. 3 into a finite dimensional matrix equation in a manner which rigorously conserves particles and energy. The dimensionality of the matrix equation is the number of mesh points over which neutral particle transport is to be calculated. In Sec. 4 we present some results and a comparison with the ANISN calculation of Gilligan et al. [7] and with results using another neutral atom transport routine (FASLAB), developed at Oak Ridge [8].

## 2. The Transport Integral Equation

We consider a slab of width  $dx$  filled with plasma as shown in Fig. 1. The plasma density and temperatures are functions of  $x$ , the coordinate normal to the slab face. We divide the neutral particles into two classes: those emitted from the wall at  $x=0$ , and those born inside the plasma by charge exchange. The latter are assumed to be born isotropically and with a single energy  $E$ , defined by the ion temperature  $T_i$  at the place of birth.

$$E = \frac{1}{2} m v^2 = \frac{3}{2} k_B T_i(x) \quad (1)$$

The neutral particles emitted by the wall are divided into discrete energy groups and have a specified angular distribution with respect to the  $x$ -axis.

We begin with the wall-originated particles. Let  $\eta(\theta)$  be the number emitted per unit wall area per unit time per unit solid angle in the direction  $\theta$ . We consider first a single energy group with energy  $E_0 = \frac{1}{2} m v_0^2$ . The number of particles traversing a differential area  $da$  (normal to the x-axis) per unit time due to source points in an annular ring of width  $dr$  and radius  $r$ , as shown in Fig. 2, is

$$\frac{dN}{dt} = \eta(\theta) 2\pi r dr d\Omega e^{-\int_0^s \frac{\mu_0(x', E_0)}{v_0} ds'} \quad (2)$$

where  $d\Omega = da \cos\theta/s^2$ . The exponential factor is due to absorption along the path length  $s$ , and

$$\mu_0(x, E_0) = n_e(x) \langle\sigma v\rangle_e + n_i(x) [\langle\sigma v\rangle_i + \langle\sigma v\rangle_{cx}] \quad (3)$$

The reaction rates for electron impact ionization,  $\langle\sigma v\rangle_e$ , ion impact ionization,  $\langle\sigma v\rangle_i$ , and charge exchange,  $\langle\sigma v\rangle_{cx}$ , depend on  $x$  through the electron temperature  $T_e(x)$ , and the ion temperature  $T_i(x)$ , and on the neutral energy  $E_0$ .  $n_e(x)$  and  $n_i(x)$  are, of course, the electron and ion density, respectively. Since  $x = s \cos\theta$ ,

$$\int_0^s \frac{\mu_0(x', E_0)}{v_0} ds' = \frac{1}{\cos\theta} \int_0^x \frac{\mu_0(x', E_0) dx'}{v_0} = \frac{\beta_0(x)}{\cos\theta} \quad (4)$$

$\beta_0(x)$  being the optical depth.

To obtain the neutral particle flux  $\Gamma$  traversing  $da$ , we integrate (2) over  $r$  and divide by  $da$ ;

$$\Gamma = 2\pi \int_0^\infty r dr \frac{\eta(\theta) \cos\theta}{s^2} e^{-\beta_0(x)/\cos\theta}$$

It is more convenient to integrate over  $u$ , rather than  $r$ , where  $u = 1/\cos\theta$ .

The flux  $\Gamma$  then becomes

$$\Gamma = 2\pi \int_1^\infty du \frac{\eta(\theta(u))}{u^2} e^{-\beta_0 u} \quad (5)$$

We consider now two cases. First, let the source function  $\eta(\theta)$  be isotropic ( $\eta(\theta) = \eta$ ). Then

$$\Gamma = 2\pi\eta E_2(\beta_0(x))$$

where

$$E_n(z) = \int_1^\infty \frac{e^{-zt} dt}{t^n} \quad (6)$$

is the exponential integral [9]. Noting that  $2\pi\eta = \Gamma_0$ , the flux at  $x = 0$ , we can write  $\Gamma(x)$  as

$$\Gamma(x) = \Gamma_0 E_2(\beta(x)) \quad (7)$$

For the second case we consider a  $\cos\theta$  source ( $\eta(\theta) = \eta_1 \cos\theta$ ). Then we get

$$\Gamma(x) = 2 \Gamma_0 E_3(\beta(x)) \quad (8)$$

as the expression equivalent to (7) for this case. (Recall that  $E_3(0) = 1/2$ ,  $E_2(0) = 1$ ).

For the wall originated neutral particles, we use eq. (8), corresponding to a  $\cos\theta$  angular distribution of the source. This is equivalent to assuming that these particles have an isotropic distribution function at  $x = 0$ . The first case, isotropic source, will be used for the internally born particles.



The absorption rate per unit volume in the plasma is

$$A(x) = - \frac{d\Gamma}{dx} \quad (9)$$

and the fraction of the absorption rate due to charge exchange is  $n_i \langle \sigma v \rangle_{cx} / \mu(x, E_0)$ . Each charge exchange event produces a first generation neutral particle in the plasma. Thus,

$$S_1(x) = \frac{n_i(x) \langle \sigma v \rangle_{cx}}{\mu_0(x, E_0)} A(x)$$

is the source rate for first generation internally born neutral particles. We can rewrite this expression as

$$S_1(x) = 2 \frac{n_i(x) \langle \sigma v \rangle_{cx}}{v_0} E_2(\beta_0(x)) \Gamma_0 \quad (10)$$

To obtain the total source rate for first generation neutrals, we write eq. (10) for each energy group and sum over groups.

Let us now consider the internally born neutral particles. Let  $S_p(x)$  be the source function for the  $p$ 'th generation. At each possible birth point  $x$ , they are assumed to be born isotropically and with a single energy  $E(x) = \frac{3}{2} k_B T_i(x) = \frac{1}{2} m v^2(x)$ . Consider a slab of thickness  $dx'$  at  $x'$  (See Fig. 1); the flux of particles at  $x (x > x')$  due to the source in the slab at  $x'$  is

$$d\Gamma_p^r(x) = \frac{1}{2} S_p(x') E_2(\beta(x', x)) dx' \quad (11)$$

by application of eq. (7). The  $r$  superscript denotes that these particles are travelling to the right at  $x$  and the  $\frac{1}{2}$  arises because only half of the particles born at  $x'$  go to the right (i.e.,  $v_x > 0$ ). Also

$$\beta(x', x) = \left| \int_{x'}^x \frac{\mu(x'', x')}{v(x')} dx'' \right| \quad (12)$$

and

$$\mu(x'', x') = n_e(x'') \langle \sigma v \rangle_e + n_i(x'') [\langle \sigma v \rangle_i + \langle \sigma v \rangle_{cx}] \quad (13)$$

The arguments of the reaction rates in (13) are  $T_e(x'')$  for  $\langle \sigma v \rangle_e$  and  $(T_i(x''), E(x'))$  for  $\langle \sigma v \rangle_i$  and  $\langle \sigma v \rangle_{cx}$ ; the absolute value sign has been introduced in (12) for convenience later.

We now differentiate  $d\Gamma_p^r(x)$  with respect to  $x$  to obtain the absorption rate at  $x$  due to the particles born in  $dx'$  and multiply this by  $n_i(x) \langle \sigma v \rangle_{cx} \mu^{-1}$  to get the charge exchange rate at  $x$ . This gives us the contribution to the source rate at  $x$  of the  $(p+1)$ 'th generation due to the  $p$ 'th generation at  $x'$ . We also have a similar expression for the particles travelling to the left at  $x$ ; they were born at  $x' > x$ . The total source rate  $S_{p+1}$  is then found by integrating over  $x'$ . We get

$$S_{p+1}(x) = \int_0^d dx' K(x, x') S_p(x') \quad (14)$$

where the kernel  $K(x, x')$  is given by

$$K(x, x') = \frac{1}{2} \frac{n_i(x) \langle \sigma v \rangle_{cx}}{v(x')} E_1(\beta(x', x)) \quad (15)$$

where  $\beta(x', x)$  is given by (12) for both  $x' < x$  and  $x' > x$ .

The interesting property of (14) and (15) is that the kernel is independent of the generation. It is convenient to write (14) symbolically as

$$S_{p+1}(x) = K S_p(x) \quad (16)$$

where  $K$  is the integral operator whose kernel is given by (15). The total charge exchange rate per unit volume  $S(x)$  is found by summing over generations;

$$\begin{aligned} S(x) &= \sum_{p=1}^{\infty} S_p(x) \\ &= (I + K + K^2 + K^3 + \dots) S_1(x) \\ &= \frac{1}{I - K} S_1(x) \end{aligned}$$

using (16) recursively. We can rewrite this expression as

$$S(x) = S_1(x) + K S(x) ,$$

which, when written out explicitly, is

$$S(x) = S_1(x) + \int_0^d dx' K(x, x') S(x') \quad (17)$$

This is an integral equation determining the total charge exchange rate per unit volume  $S(x)$  in the plasma; the inhomogeneous term  $S_1(x)$  is given by eq. (10). From the function  $S(x)$  one can determine all other quantities of interest. For example, the ionization rate due to electron impact is

$$S_e(x) = \int_0^d dx' \frac{n_e(x) \langle \sigma v \rangle_e}{n_i(x) \langle \sigma v \rangle_{cx}} K(x, x') S(x') \\ + \frac{n_e(x) \langle \sigma v \rangle_e}{n_i(x) \langle \sigma v \rangle_{cx}} S_1(x) , \quad (18)$$

the energy loss rate due to charge exchange is

$$W_{cx}(x) = \int_0^d dx' \frac{3}{2} k_B [T_i(x) - T_i(x')] K(x, x') S(x') \\ + \left[ \frac{3}{2} k_B T_i(x) - E_0 \right] S_1(x) \quad (19)$$

and the neutral particle flux incident on the wall is

$$\Gamma_w = \int_0^d dx \frac{1}{2} S(x) E_2(\beta(0, x)) . \quad (20)$$

The integrand in (20) has an interesting significance. It is the source rate of particles that reach the wall without further collision. From this source rate and the temperature profile, one can construct the energy distribution of the neutral particles incident on the wall. This will be discussed further in the next section. The neutral particle density profile in the plasma is most easily found from the electron impact ionization rate. Since  $\langle \sigma v \rangle_e$  is essentially independent of the neutral particle energy, but is a function of  $T_e(x)$  we can write

$$S_e(x) = n_i(x) n_0(x) \langle \sigma v \rangle_e \quad (21)$$

Hence the neutral particle density  $n_0(x)$  can be obtained from (18) and (21).

### 3. The Discretized System

We consider in this section the reduction of the integral equation (18) to a finitely dimensioned matrix equation which is then solved by a single matrix inversion. The scheme used for reducing the integral equation to the matrix equation is based upon the application we have in mind: use as a neutral transport routine in the WHIST code [10], which is a Tokamak simulation code. This scheme has the property that it explicitly conserves particles and energy, regardless of the mesh spacing.

We consider a set of mesh points  $j$  with coordinates  $x_j$  ( $j = 1, N$ ) and associated zones, as shown in Fig. 3. The boundaries between the zones are midway between meshpoints (which may be nonuniformly spaced). The zone widths are  $\Delta_j = (x_{j+1} - x_{j-1})/2$ . This is the mesh-zone configuration used in the WHIST code for the plasma transport equations. The required plasma data is given at the meshpoints  $j$ .

The reduction scheme consists of calculating, for a given generation, the flux (of the particles travelling to the right, for example) entering and leaving each zone. This difference represents the net absorption in that zone; a certain fraction of it is due to charge exchange and represents the source for the next generation. This source is assumed to be concentrated at the meshpoints. A higher order approximation would be to assume that the charge exchange source is uniform inside a given zone; the error is small if the zone widths are small compared with the neutral mean free path. This scheme was used earlier by Khelladi [11] in another neutral transport routine based on following generations.

We consider first the neutral particles streaming from the wall. The optical depth to the left face of the  $j$ 'th zone is

$$\beta_j^0 = \sum_{i=1}^{j-1} \frac{\mu(x_i, E_0)}{v_0} \Delta_i$$

The absorption rate per unit volume in the  $j$ 'th zone is

$$A_j = 2\Gamma_0 \frac{E_3(\beta_j^0) - E_3(\beta_{j+1}^0)}{\Delta_j}$$

Hence the source for the first generation of internally born neutral particles is

$$S_1(x_j) = 2\Gamma_0 \frac{n_i(x_j) \langle \sigma v \rangle_{cx}}{\mu(x_j, E_0) \Delta_j} [E_3(\beta_j^0) - E_3(\beta_{j+1}^0)] \quad (22)$$

This is the discretized version of eq. (10). Here,  $\langle \sigma v \rangle_{cx}$  has as argument  $(T_i(x_j), E_0)$ .

We follow a similar procedure for the internally born neutral particles. In this case the optical depths are calculated between the  $k$ 'th meshpoint and the two faces of the  $j$ 'th zone. Let us introduce the shorthand notation  $v_j = v(x_j)$ ,  $\mu_{jk} = \mu(x_j, x_k)$ . Then

$$v_k \beta_{jk}^- = \sum_{i=k+1}^{j-1} \mu_{ik} \Delta_i + \frac{1}{2} \mu_{kk} (x_{k+1} - x_k) \quad (23)$$

if  $j > k$ , and

$$v_k \beta_{jk}^- = \sum_{i=j+1}^{k-1} \mu_{ik} \Delta_i + \frac{1}{2} \mu_{kk} (x_k - x_{k-1}) \quad (24)$$

if  $k > j$ . We also define

$$\beta_{jk}^+ = \beta_{jk}^- + \frac{\mu_{jk} \Delta_j}{v_k} \quad (25)$$

Clearly  $\beta_{jk}^-$  is the optical depth to the near face of the j'th zone and  $\beta_{jk}^+$  is the optical depth to the far face.

The absorption rate in the j'th zone due to the source in the k'th zone is

$$A_{jk} = \frac{1}{2} \frac{S_p(x_j) \Delta_k}{\Delta_j} [E_2(\beta_{jk}^-) - E_2(\beta_{jk}^+)]$$

for  $k \neq j$ . For  $k = j$ , the flux out the right face is

$$\Gamma_r = \frac{1}{2} S_p(x_j) \Delta_j E_2(\beta_j^r),$$

and out the left face is

$$\Gamma_\ell = \frac{1}{2} S_p(x_j) \Delta_j E_2(\beta_j^\ell),$$

where

$$\beta_j^r = \frac{\mu_{jj}(x_{j+1} - x_j)}{2v_j} \quad (26)$$

$$\beta_j^\ell = \frac{\mu_{jj}(x_j - x_{j-1})}{2v_j} \quad (27)$$

The absorption rate in the j'th zone due to the particles born in the same zone is

$$A_{jj} = S_p(x_j) - \frac{(\Gamma_r + \Gamma_\ell)}{\Delta_j}$$

which becomes

$$A_{jj} = \frac{1}{2} S_p(x_j) [2 - E_2(\beta_j^r) - E_2(\beta_j^l)]$$

We multiply the absorption rate  $A_{jk}$  by the probability that the absorption was due to charge exchange and sum over the source slabs  $k$  to get the source for the next generation. We obtain the result

$$S_{p+1}(x_j) = \sum_k K_{jk} S_p(x_k) \quad (28)$$

where

$$K_{jk} = \frac{1}{2} \frac{n_i(x_j) \langle \sigma v \rangle_{cx}}{\mu_{jk}} \frac{\Delta_k}{\Delta_j} [E_2(\beta_{jk}^-) - E_2(\beta_{jk}^+)]$$

if  $j \neq k$ , and

(29)

$$K_{jj} = \frac{1}{2} \frac{n_i(x_j) \langle \sigma v \rangle_{cx}}{\mu_{jj}} [2 - E_2(\beta_j^r) - E_2(\beta_j^l)]$$

if  $j = k$ .

The matrix  $K_{jk}$  is the discretized form of the integral operator  $K$  defined in eq. (14). The optical depths needed in the calculation of  $K_{jk}$  are given in eqs. (23) - (27).

In the same way as in the continuous system, one sums over generations to get the total charge exchange rate per unit volume. This is determined by the matrix equation

$$\vec{S} = \vec{S}_1 + \vec{K} \cdot \vec{S},$$

which has the solution

$$\vec{S} = (\vec{I} - \vec{K})^{-1} \cdot \vec{S}_1 \quad (30)$$



The neutral particle code SPUDNUT calculates the vector  $\vec{S}_1$  (determined by the wall-originated particles), the matrix  $\vec{K}$ , and then calculates  $\vec{S}$  by computing the inverse  $(\vec{I} - \vec{K})^{-1}$ . The inversion routine used is due to Crout [12]. The particle source and energy sink terms needed by the plasma transport equations are then calculated by matrix operations using  $\vec{S}$ . If desired, one can also calculate the neutral density, as well, from  $\vec{S}$ . For completeness, we list here the matrix equations for these source and sink terms.

Electron impact ionization rate:

$$S_e(x_j) = \sum_k \frac{n_e(x_j) \langle \sigma v \rangle_e}{n_i(x_j) \langle \sigma v \rangle_{cx}} K_{jk} S(x_k) + \frac{n_e(x_j) \langle \sigma v \rangle_e}{n_i(x_j) \langle \sigma v \rangle_{cx}} S_1(x_j). \quad (31)$$

Ion impact ionization rate:

$$S_i(x_j) = \sum_k \frac{n_i(x_j) \langle \sigma v \rangle_i}{n_i(x_j) \langle \sigma v \rangle_{cx}} K_{jk} S(x_k) + \frac{n_i(x_j) \langle \sigma v \rangle_i}{n_i(x_j) \langle \sigma v \rangle_{cx}} S_1(x_j). \quad (32)$$

Energy loss rate from the ions due to charge exchange

$$\begin{aligned} W_{cx}(x_j) = & \frac{3}{2} k_B \sum_m [T_i(x_j) - T_i(x_m)] K_{jm} S(x_m) \\ & + \left[ \frac{3}{2} k_B T_i(x_j) - E_0 \right] S_1(x_j). \end{aligned} \quad (33)$$

Kinetic energy deposition in the ions due to ionization:

$$\begin{aligned}
 W_i(x_j) = & \sum_k \frac{n_e(x_j) \langle \sigma v \rangle_e + n_i(x_j) \langle \sigma v \rangle_i}{n_i(x_j) \langle \sigma v \rangle_{cx}} \cdot \frac{3}{2} k_B T_i(x_k) K_{jk} S(x_k) \\
 & + \frac{n_e(x_j) \langle \sigma v \rangle_e + n_i(x_j) \langle \sigma v \rangle_i}{n_i(x_j) \langle \sigma v \rangle_{cx}} \cdot E_0 S_1(x_j).
 \end{aligned} \tag{34}$$

Furthermore, one removes from the electrons an energy price for each electron impact ionization event and from the ions for each ion impact ionization event. In SPUDNUT, this energy price is chosen to be 13.6 eV, corresponding to the ionization potential, but could be set higher to phenomenologically account for excitation as well as ionization.

The flux of energetic neutrals incident on the wall is calculated using the discretized form of eq. (20).

$$\Gamma_w = \frac{1}{2} \sum_k S(x_k) E_2(\beta(0, x_k)) \tag{35}$$

where

$$\beta(0, x_k) = \sum_{i=1}^{k-1} \frac{\mu_{ik} \Delta_i}{v_k} + \frac{\mu_{kk}(x_k - x_{k-1})}{2v_k}.$$

The energy distribution of the particles hitting the wall is obtained by noting that the particles belonging to each term in the summation in eq. (35) have an energy  $E_k = \frac{3}{2} k_B T_i(x_k)$ .

Reflection of energetic particles at the wall can be easily incorporated in the routine by introducing an energy dependent reflection coefficient [13] and a prescription for dividing the reflected particles into the various energy groups comprising the flux  $\Gamma_0$  of particles entering the plasma. The outgoing fluxes are then calculated iteratively until the results converge. Since this is external to the basic neutral particle transport routine, it is not discussed further here.

#### 4. Comparative Calculations

Multigroup ANISN calculations of the neutral particle transport were reported by Gilligan [7] for the TFTR plasma. For these calculations the plasma density and temperatures were taken to be

$$n_i(x) = n_i(0)[1 - (\frac{r}{a})^3] + n_i(a)$$

$$T_e(x) = T_i(x) = T_i(0)[1 - (\frac{r}{a})^2] + T_i(a)$$

where  $n_i(0) = 4 \times 10^{13}$ ,  $T_i(0) = 9550$  eV,  $T_i(a) = 50$  eV. The effective cold neutral particle density at the edge (.5\* physical gas density) was taken to be  $5 \times 10^9 \text{ cm}^{-3}$  (yielding a flux into the plasma given by the expression

$\Gamma = (\frac{n_{\text{eff}} v}{2})$  with an energy of 3 eV. Using these parameters, the same calculation was done using SPUDNUT and FASLAB. The neutral density profile obtained by each of the routines is shown in Fig. 4. As can be seen, significant differences in the neutral density, as calculated by the three different codes, appear only after the neutral density has been attenuated by more than two orders of magnitude. This difference is not generally significant in tokamak simulation codes; the interesting region is the first two orders of magnitude. The energetic neutral particles reaching the wall are born primarily in this region. Furthermore, the neutral particle effects in the plasma transport equations are significant only in this zone (i.e., near the edge of the plasma). The energy spectrum of the energetic neutral particle flux incident on the wall is shown in Fig. 5 for the ANISN and SPUDNUT calculations; again the agreement is good.

The ANISN calculation took 75 sec on an IBM 360/91 [7], compared to 1.35 sec for FASLAB and .06 sec for SPUDNUT, both on the CDC-7600.

A comparison has also been made for a reactor size plasma, NUWMAK [14], using FASLAB and SPUDNUT. In this case the assumed plasma density and temperature are

$$n_i(x) = n_e(x) = n(0)[1 - (\frac{r}{a})^2] + n(a)$$

$$T_e(x) = T_i(x) = T_i(0)[1 - (\frac{r}{a})^2] + T_i(a) ,$$

where  $n(0) = 1.95 \times 10^{14}$ ,  $n(a) = 3.2 \times 10^9$ ,  $T_i(0) = 10$  keV,  $T_i(a) = 30$  eV.

The effective cold neutral density at the edge is  $1.9 \times 10^{10}$  and their energy is 5 eV. The neutral particle density is shown in Fig. 6., the ionization rate in Fig. 7, and the energy loss rate from the ions in Fig. 8. The solid lines are for no particle reflection at the wall, and the dotted line is for particle reflection. Particle reflection does not make a significant difference, at least in these calculations. The agreement between the two codes is good.

Shown in Fig. 9 is the source rate for neutral particles that reach the wall without further collisions, and in Fig. 10 is their energy spectrum (normalized to unity). The total particle flux incident on the wall is  $\Gamma_w = 8.5 \times 10^{15}$ , as calculated by SPUDNUT, and  $\Gamma_w = 7.5 \times 10^{15}$ , as calculated by FASLAB.

## 5. The Subroutine SPUDNUT

In this section a detailed description of the subroutine is given. Sections 5.1.1 and 5.1.2 describe a way of indexing certain variables which allows for considerable savings in core space and execution time. In section 5.2 the structure of the subroutine and its particle and energy balances are discussed. Later sections contain lists of common blocks, variables and subroutines called.

### 5.1.1 Indexing of Local Variables

Variables that are relevant outside SPUDNUT are labeled with an index  $i$  (or  $il$ ), counting from 1 at the center through  $N$  just outside it. Recall that the plasma boundary is located between the meshpoints  $N-1$  and  $N$ . Variables local to SPUDNUT have an index  $J$  (or  $Jl$ ) counting from 1 at  $X_{N-1}$  to NMD at a specified point in the plasma. This means that these variables are only defined where they are actually required, i.e., in the area to which the neutral calculation is restricted.

### 5.1.2 Indexing of Cross-Sections and Energy Groups

When calculating the various cross-sections, three distinct types of energies play a role:

- (1) at every one of the NMD meshpoints, particles can originate from all these meshpoints, having the corresponding energies,
- (2) the energy groups in which the flux from the wall is divided number  $NMD/2$  ( $= NSC$ ) and are chosen such as to make their energies coincide with these corresponding to the temperatures at the odd meshpoints, counting inwards on the  $J$ -scale,
- (3) an extra energy group is allocated to the external influx. Hence the cross-sections have dimension  $NMD \times (NMD+1)$  while the flux from the wall (FWALL) and its energies (ENS) are dimensioned  $NSC+1$ .

## 5.2 Structure of the Subroutine

The structure of the program is very straightforward, containing only a single iterative loop. The table below lists the most relevant sections, an \* identifying the sections inside the iterative loop. The variable TOL, which serves to decide on the convergence of the latter, and KSPUT which indicates whether or not the subroutine ALBDST (see Section 5.5) is called, are the only arguments of SPUDNUT.

STMNT	Calculates
51 - 62	cross-sections
71 - 120	kernel AKCX
124 - 146	Crout decomposition of AKII
* 159 - 187	initial SCXØ, SION, VTE, VII, (DENØ)
* 193 - 208	SORCX
* 210 - 247	final SION, VTE, VII, ALBEDØ, (ALBEDI), (DENØ)
* 252	call BKSCAT
* 253 - 262	convergence test
274	call ALBDST

The statements 224-235, calculating the inwards escape rate ALBEDI and 180-187/244-247 where the neutral density DENØ is calculated are optional and should not be included when the subroutine is used as a part of the transport codes WHIST or CRIST (version 53 or later).

Particle and energy balances can be tested according to:

$$\sum_k \text{FWALL}(k) = \sum_i [\text{SION}(i) + \text{ALBEDO}(i) + \text{ALBEDI}(i)] * \text{DR}(i)$$

and

$$\begin{aligned} \sum_k \text{FWALL}(k) * \text{ENS}(k) + 1.5 \sum_i [\text{VTI}(i) * \text{DENP}(i) + \text{VTE}(i) * \text{DEN}(i)] * \text{DR}(i) \\ = \sum_i [13.6 * \text{SION}(i) + 1.5 * \text{TI}(i) * \{\text{ALBEDO}(i) + \text{ALBEDI}(i)\}] * \text{DR}(i) , \end{aligned}$$

respectively.

### 5.3 Common Blocks

/DENH/ contains all the output variables of the subroutine, including those calculated in the subroutine BKSCAT.

FWALL(k), ENS(k): flux from the wall and its energy distribution.

The first NSC elements come from BKSCAT, the last two are actually input variables. ( $\text{\#/cm}^2\cdot\text{sec}$  and eV, respectively).

SION(i): local ionization rate ( $\text{\#/cm}^3\cdot\text{sec}$ )

VTE(i), VTI(i): local energy transfer from electrons, ions to neutrals (eV/particle $\cdot\text{sec}$ )

ALBEDO(i), ALBEDI(i): local outwards, inwards escape rate ( $\text{\#/cm}^3\text{ sec}$ )

/GEOM/ contains geometrical data (see section 2 and figs. 1-3)

R(i): meshpoints

DR(i): distance between meshpoints i and (i+1).

DDR(i): width of slab containing meshpoint i.

/INDEX/ N: number of meshpoints

NX: innermost meshpoint to which neutral calculation is extended.

NMD = N-NX; but is made even and  $\leq 22$  in the subroutine (output).

NSC = NMD/2 number of energy groups in FWALL (output).

IND: number of iterations when convergence criterion is satisfied (output).

NM1 = N-1

/DEN/: DEN(i), DENP(i), DENO(i): electron, proton and neutral density, respectively ( $\text{\#/cm}^3$ )

/TEMP/: TE(i), TI(i): electron and proton temperature, respectively (eV)

/ATOMIC/: AMZ: atomic mass number of limiter material

ZIMP: charge of nucleus of limiter material



ENFC: Franck-Condon energy (eV)  
 AI: atomic mass number of ions in cross-section calculation  
 AN: atomic mass number of neutrals in cross-section calculation  
 AMU: atomic mass number of plasma ions  
 FLUX: input to initialize the flux from the wall

#### 5.4 Local Variables

If the subroutine is used in conjunction with a code of the WHIST- or CRIST-family, these variables can be written over the main matrix containing the coefficients of the discretised equations. This use of the EQUIVALENCE feature allows for an important saving of core space.

SVIMPE( $j_1, j_2$ ), SVIMPI( $j_1, j_2$ ), SVCX( $j_1, j_2$ ): cross-sections for electron and ion impact ionization and charge exchange, multiplied by the relevant particle densities ( $n_e$  or  $n_i$ ). The index  $j_1$  localizes the event;  $j_2$  specifies the energy of the impacting neutral particle.

SVTOT( $j_1, j_2$ ): sum of the above.

AKCX( $j_1, j_2$ ): the kernel as defined in eq. 29.

VT( $j$ ): particle velocity corresponding with the ion temperature at R(i).

ENI( $j$ ), ENE( $j$ ): energies corresponding with ion, electron temperature at R(i).

AKII( $j_1, j_2$ ): identity matrix minus AKCX( $j_1, j_2$ ).

AKL( $j_1, j_2$ ), AKU( $j_1, j_2$ ): lower and upper triangular matrix resulting from the Crout decomposition of AKII( $j_1, j_2$ ).

SCXØ( $j$ ): original neutral source at R( $i$ ).

SORCX( $j$ ): final neutral source at R( $i$ ).

ASOR( $j, j'$ ): number of neutrals at  $x_j$  originating from  $x_{j'}$ , ( $\#/cm^3$ )

BETP, BETM: optical depths ( $\beta^+, \beta^-$ ).

### 5.5 Subroutines Called

SIGVE: calculates  $\langle \sigma v \rangle_e$ , the electron impact ionization rate.

Input: TE( $i$ ), ENI( $j$ ), AN

Output:  $x = \langle \sigma v \rangle_e$

SIGMAV: calculates  $\langle \sigma v \rangle_i$  and  $\langle \sigma v \rangle_{cx}$

Input: TI( $i$ ), ENI( $j$ ), AI, AN

Output:  $x = \langle \sigma v \rangle_i$ ,  $y = \langle \sigma v \rangle_{cx}$

BKSCAT: calculates the flux and energy distribution of the neutrals that are backscattered from the wall. All input and output is through common blocks. This subroutine calls the function REFL (see section 5.6).

ALBDST: calculates the energy distribution of the neutral flux escaping from the plasma, assuming that each plasma slab is characterized by a Maxwellian distribution of the slab temperature.

Input: ALBTOT, SORCX

Output: E = neutral escape flux energies, F = neutral escape flux with energies E (both dimensioned 50)

## 5.6 External Functions

EXPI2(x): calculates the exponential integral of the second order, using a polynomial approximation.

REFL (ENI(i), AMZ, AMU, ZIMP): calculates the particle reflection coefficient using data from Oen and Robinson.<sup>13</sup>

## Acknowledgments

We gratefully acknowledge stimulating discussions with Dr. H. Howe, Oak Ridge National Laboratory. We are also grateful to him for providing a copy of the code FASLAB. This work was supported by the U.S. Department of Energy.

### References

1. D. F. Düchs, D. E. Post, P. H. Rutherford, Nuclear Fusion 17 (1977), 565.
2. J. T. Hogan, "Multifluid Tokamak Transport Models", in Methods of Computational Physics (J. Killeen, ed.), Academic Press, New York 16 (1976), p. 131.
3. E. Greenspan, Nuclear Fusion 14 (1974), 771.
4. Z. El-Derini, E. M. Gelbard, Trans. Am. Nuclear Soc. 23, 45 (1976); "Neutral Transport Code in Plasma", Argonne National Laboratory Report FPP/TM-75 (1977).
5. J. H. Marable, E. M. Oblow, Nuclear Sci. Eng. 61 (1976), 90.
6. W. Pfeiffer, "Calculation of Neutral Transport in a Plasma Using A Neutron Transport Method", General Atomic Company Report GA-A13995 (1976).
7. J. G. Gilligan, S. L. Gralnick, W. G. Price, Jr., T. Kammash, Nuclear Fusion 18 (1978), 63.
8. H. Howe, private communication.
9. M. Abramowitz and I. A. Stegun, Handbook of Mathematical Functions, National Bureau of Standards, U.S. Government Printing Office, Washington, D.C. 20402.
10. W. A. Houlberg, R. W. Conn, Nuclear Science and Engineering 64 (1977), 141.
11. M. Khelladi, private communication.
12. P. D. Croust, Trans. AIEE 60 (1941), 1235.
13. O. S. Oen, M. T. Robinson, Nuclear Instrum. and Meth. 132 (1976), 647.

14. R. W. Conn, G. L. Kulcinski, C. W. Maynard, Trans. 3rd Topical Meeting on the Technology of Controlled Nuclear Fusion (May 9-11, 1978, Santa Fe, New Mexico) p. 351.

Figure Captions

- Fig. 1 The slab geometry for the neutral particle transport code.
- Fig. 2 Coordinates for the integration to obtain the flux of particles through the area  $da$ .
- Fig. 3 Numbering scheme for meshpoints and zones in the discretized version.
- Fig. 4 Neutral density profile in the TFTR calculation.
- Fig. 5 Energy spectrum of the neutral particle flux incident on the wall - TFTR case.
- Fig. 6 Neutral particle density in the NUWMAK calculation.
- Fig. 7 Ionization rate per unit volume - NUWMAK case.
- Fig. 8 Ion energy loss rate per unit volume - NUWMAK case.
- Fig. 9 The source rate for particles that reach the wall without further collisions - NUWMAK case.
- Fig. 10 The energy spectrum of the particle flux incident on the wall - NUWMAK case.

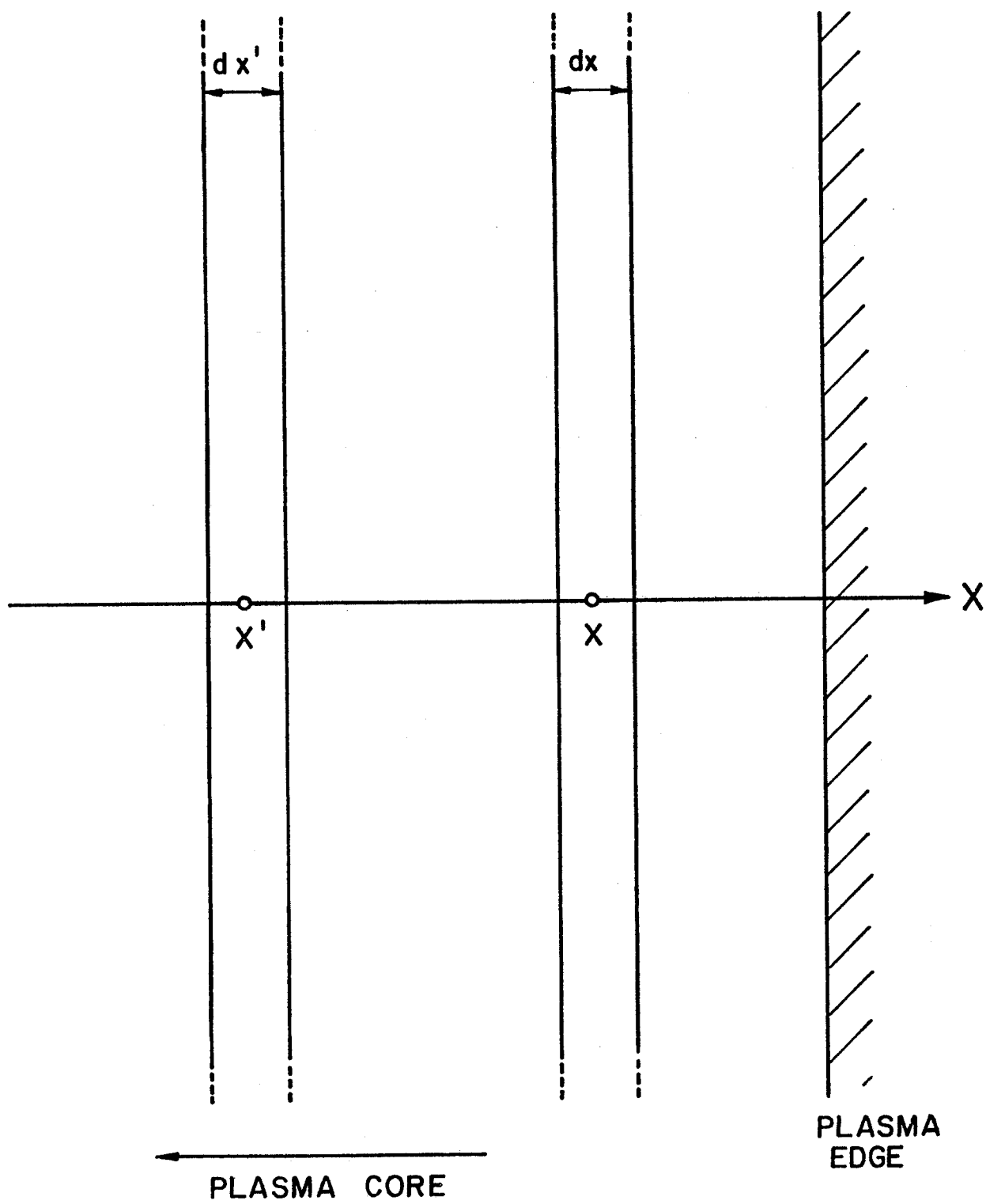


FIGURE 1

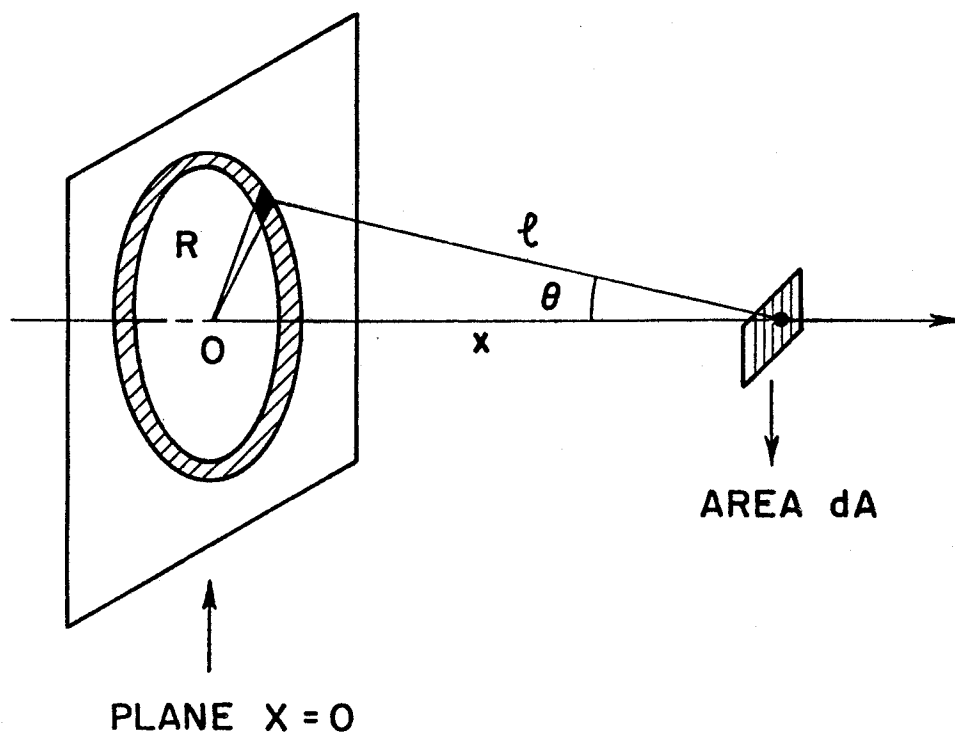


FIGURE 2



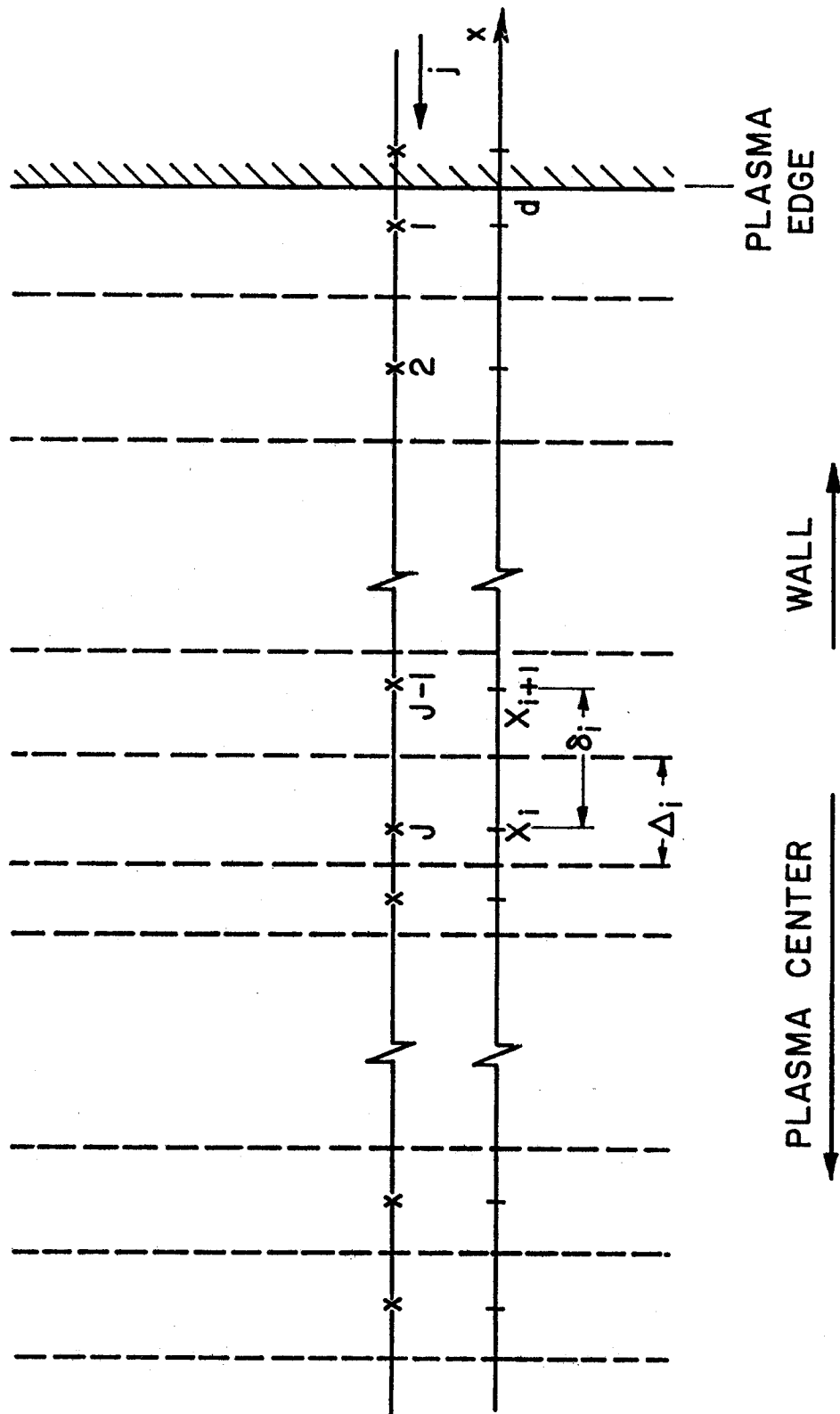


FIGURE 3

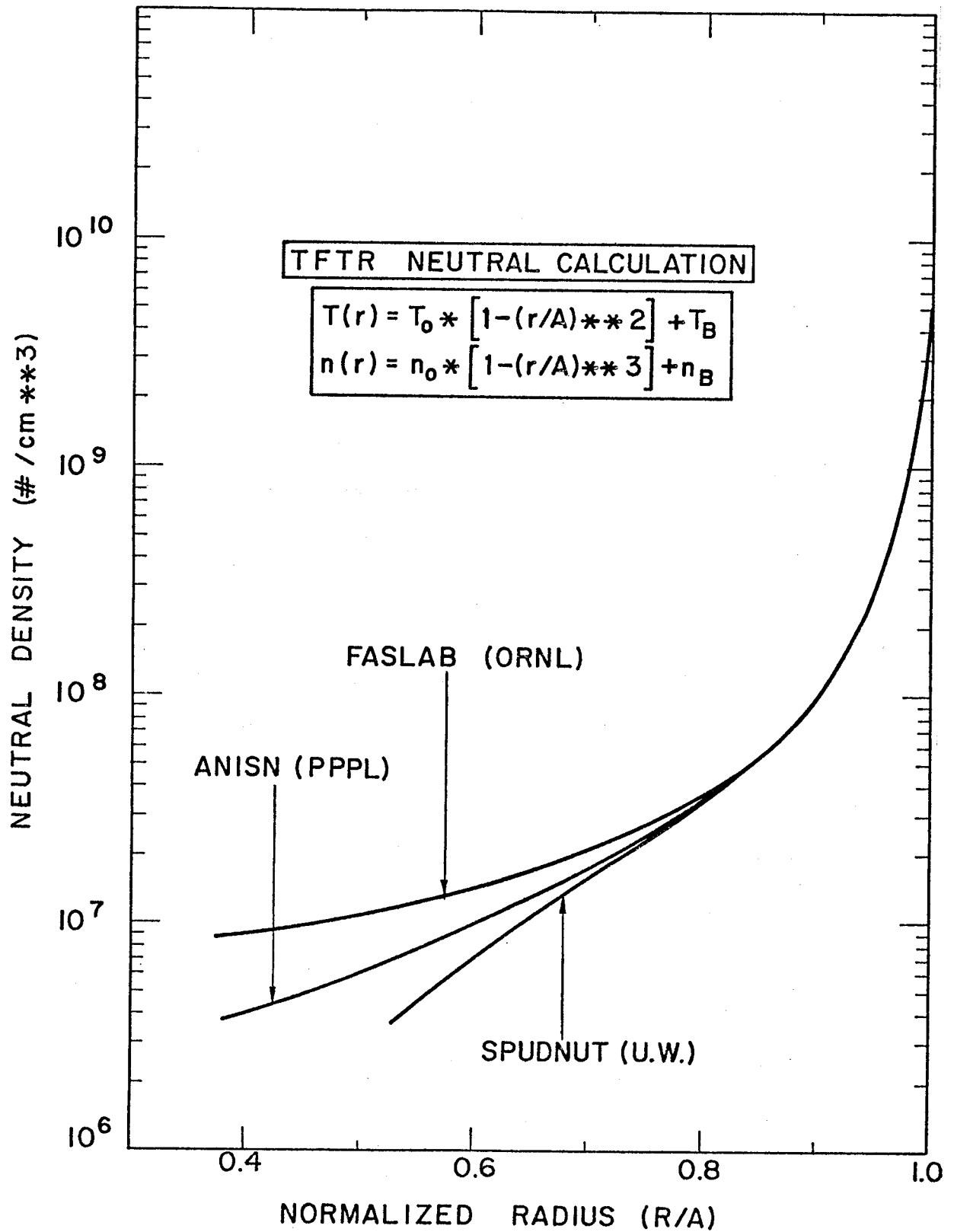


FIGURE 4

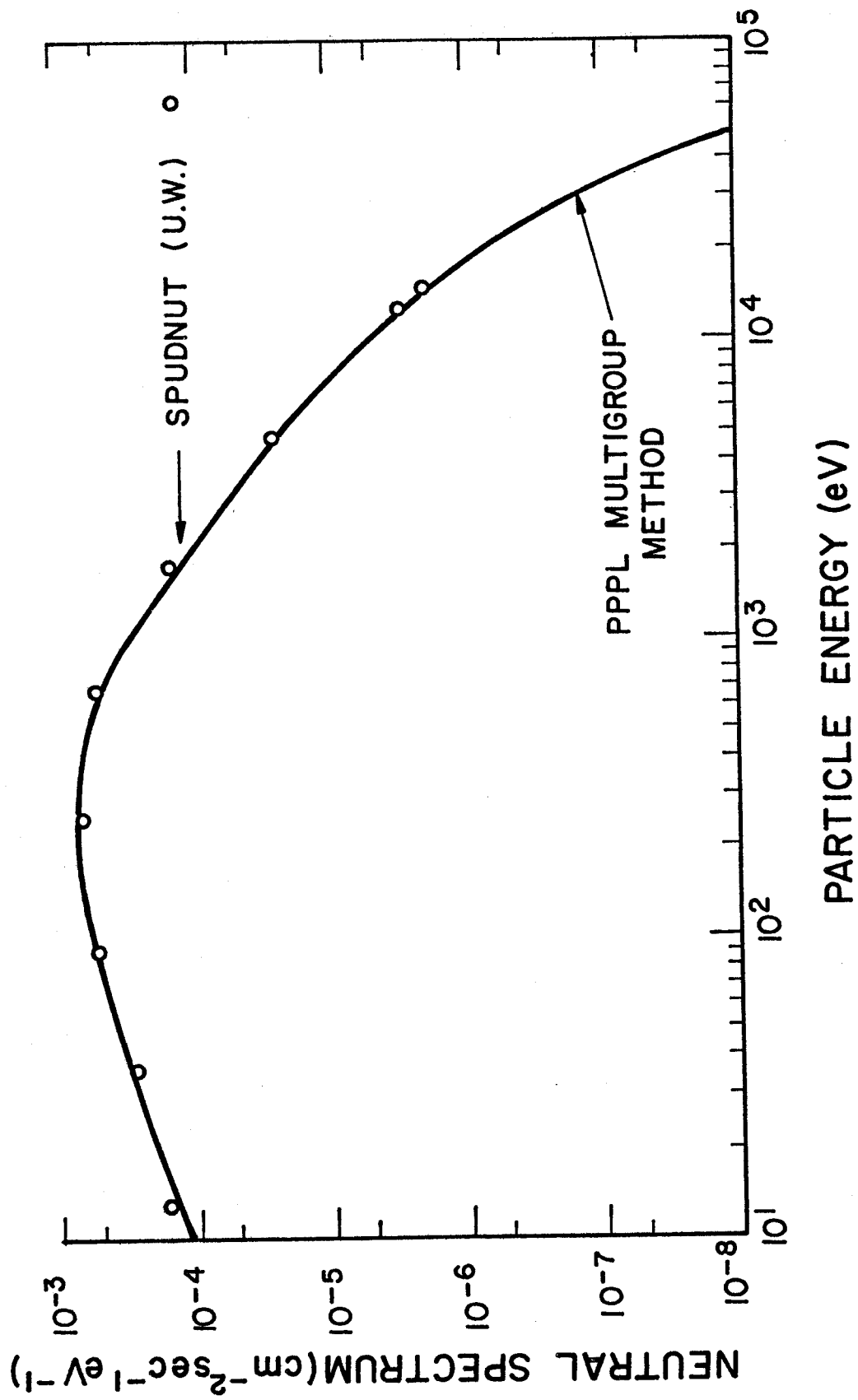


FIGURE 5

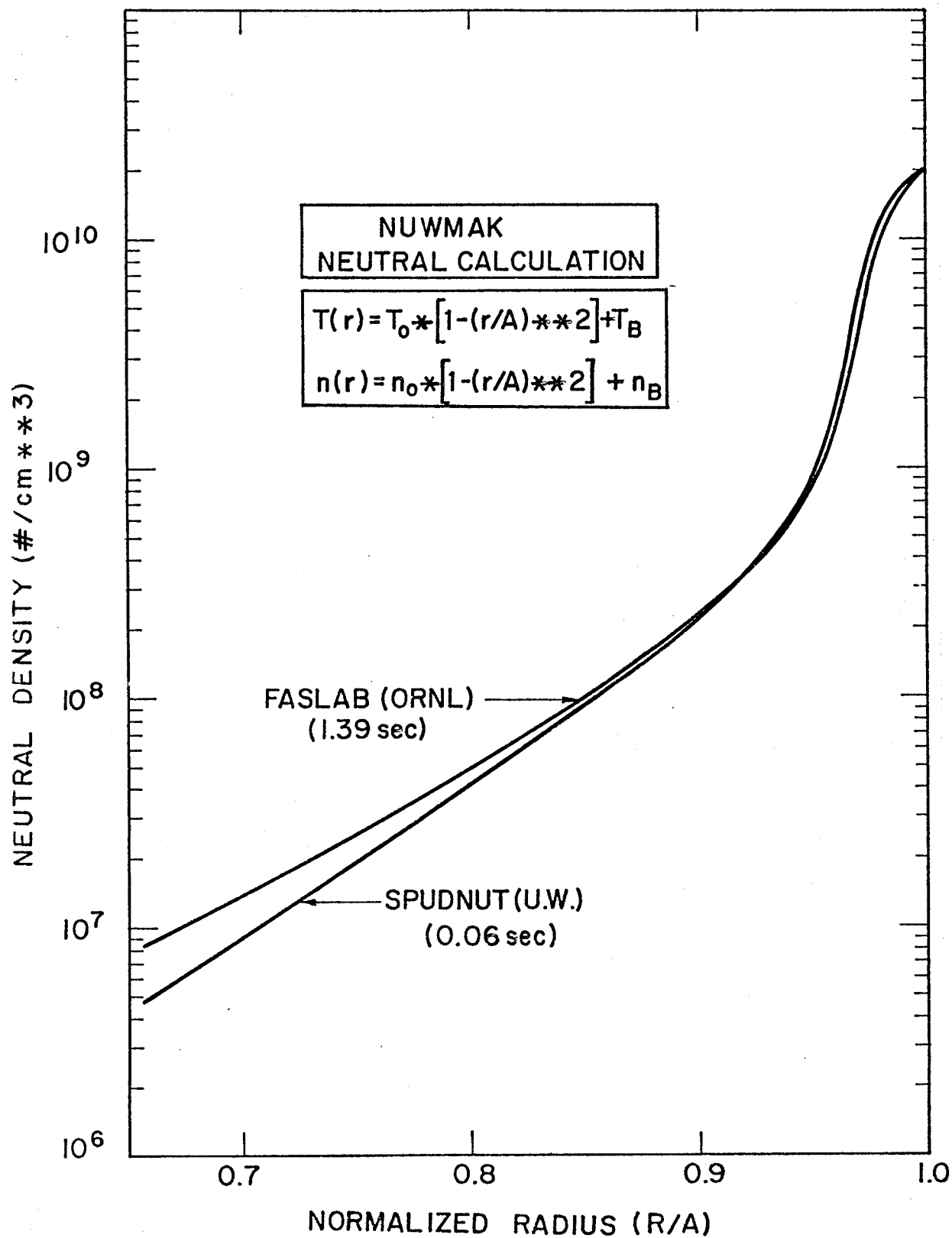


FIGURE 6

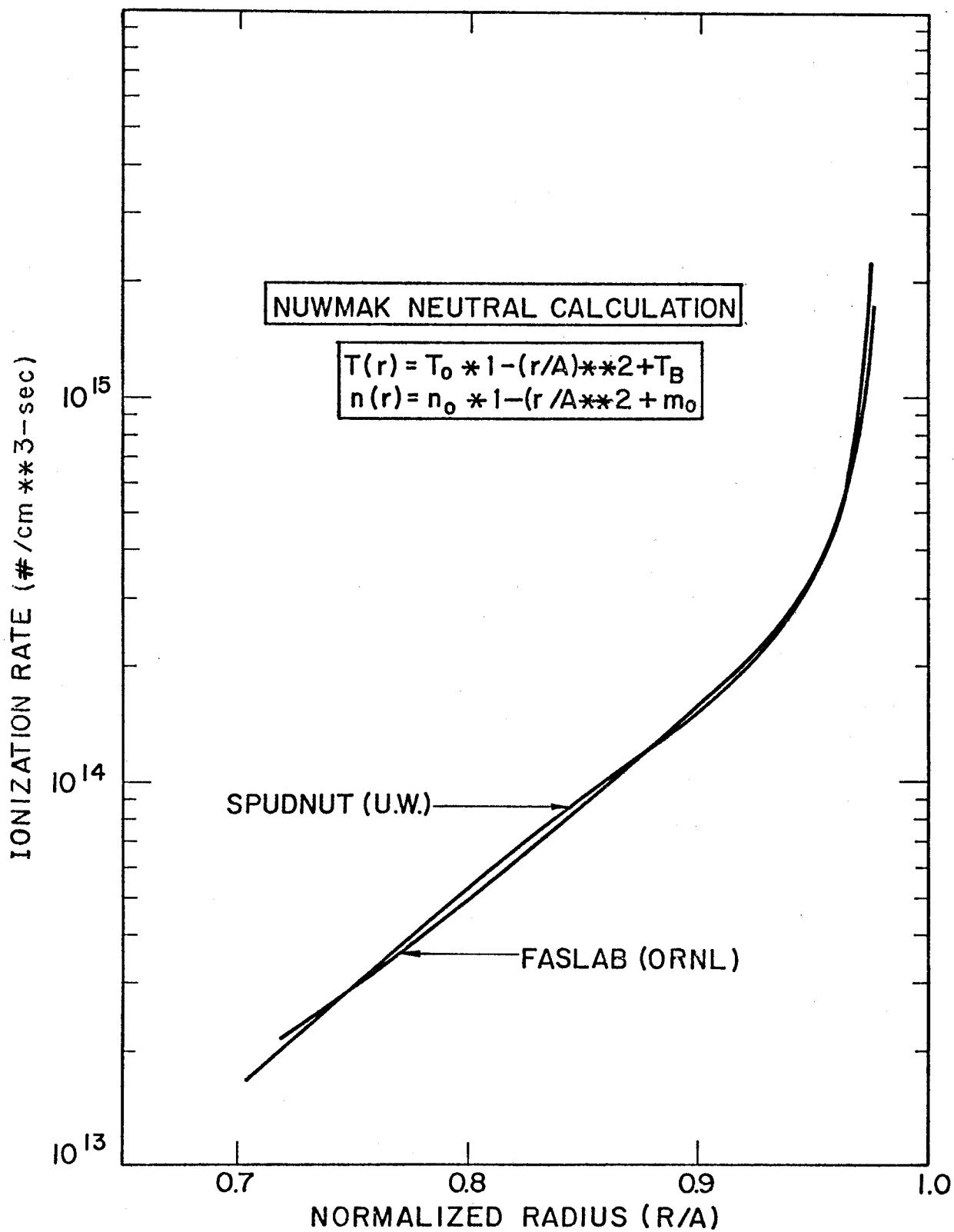


FIGURE 7

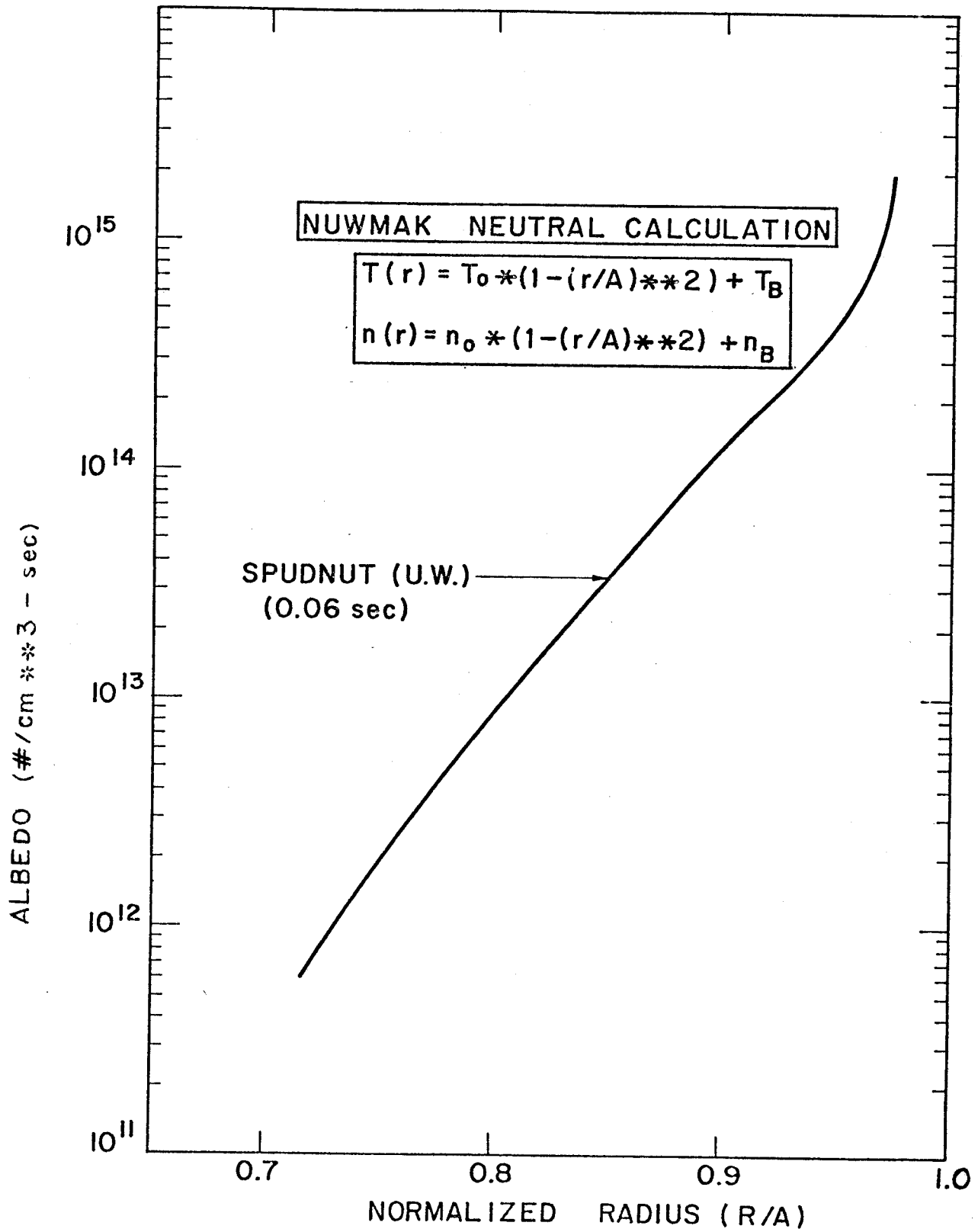


FIGURE 8

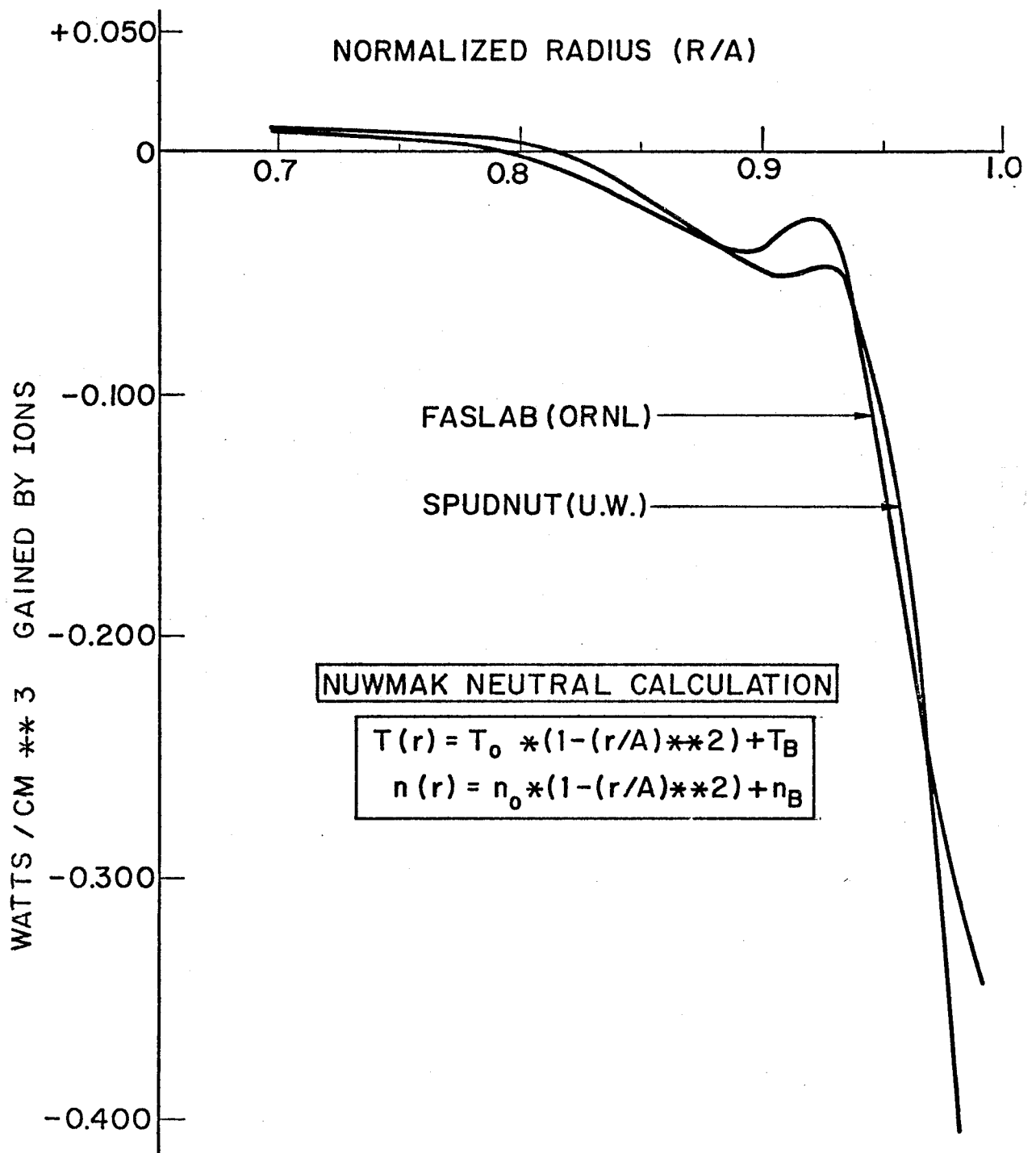


FIGURE 9

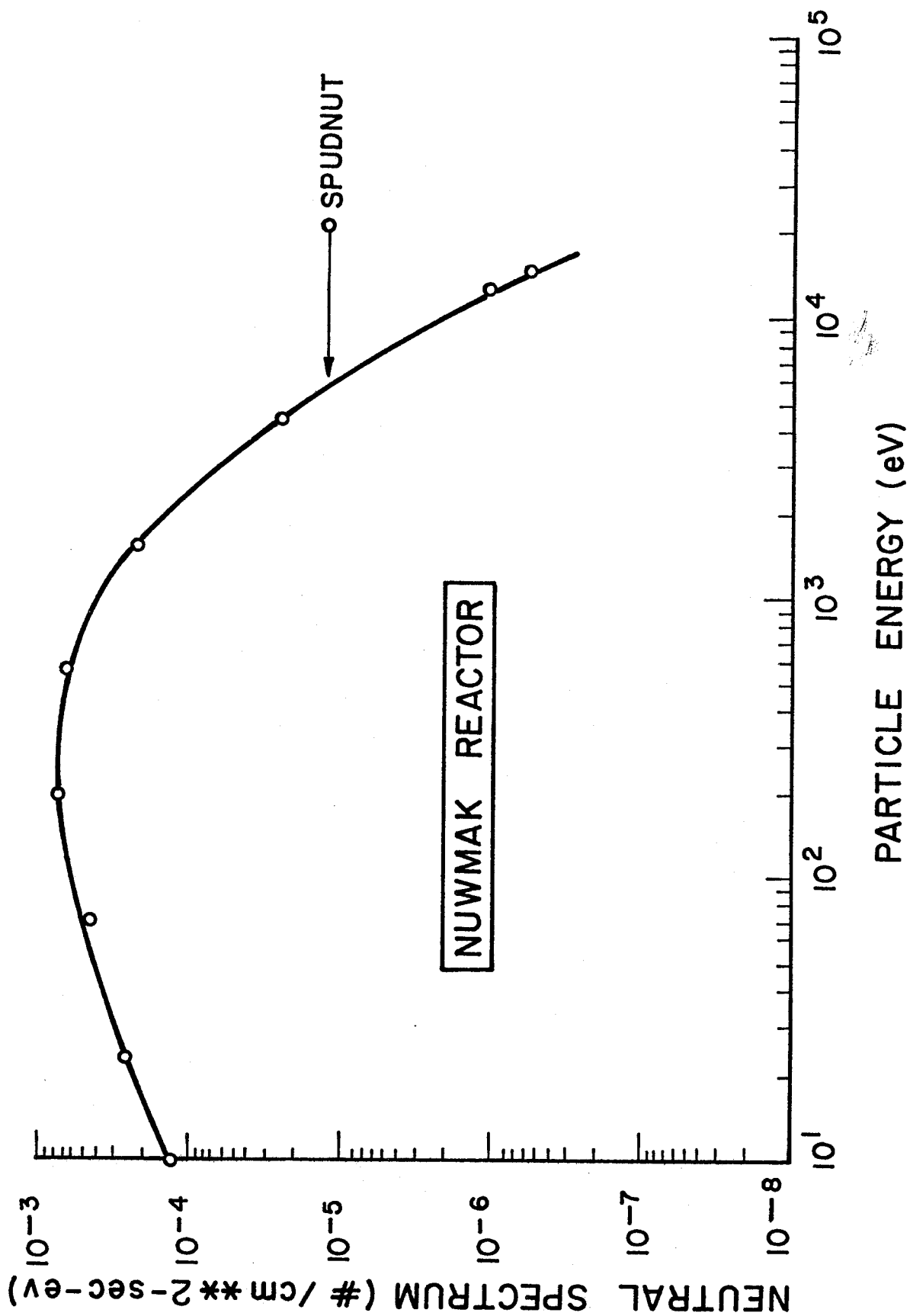


FIGURE 10